LCLS-II Technical Note

HGHG Seeding options for LCLS-II

LCLS-II TN-14-13

12/2/2014

E. Allaria, W. Fawley, Z. Huang, G. Penn

1 Introduction

The baseline LCLS-II design will implement self-seeding in the SXR and HXR for X-ray wavelengths between 0.2 and 1.3 keV and from 4 to about 12 keV. These self-seeding insertions will be similar to those that are being developed for the LCLS. An R&D program will develop self-seeding techniques for the intermediate range between 1.3 keV and 4 keV. Space is available in the SXR and HXR undulators to accommodate this planned upgrade.

External seeding, in principle, can offer many advantages over self-seeding, including better synchronization with an external laser signal for pump-probe experiments, detailed control of the temporal and spectral properties of the output pulses, and shorter total undulator lengths to reach the same saturated power levels. Over the past year, the seeded FERMI FEL at Trieste [1] has produced transversely– and longitudinally–coherent output pulses at the 10 microjoule energy level down to 5 nm wavelength, utilizing the fresh bunch technique in a two-stage, HGHG configuration (High-Gain Harmonic Generation). FERMI's near-term goal is to reach the carbon K-edge at 280 eV with its 1.5 GeV electron beam. Reaching even shorter output wavelengths (*e.g.*, 2 nm or shorter) with good longitudinal coherence is very challenging but may be feasible with the brighter and more energetic LCLS-II electron beams. The goal of this section is to show a preliminary design of a two-stage HGHG that satisfies the following criteria:

- Nearly transform-limited soft X-ray pulses over an initial range of 250 eV to 600 eV photon energy (5 nm to 2 nm radiation wavelength).
- Length of the entire FEL line of less than 80 m, allowing placement in the existing End-Station A (ESA) tunnel.
- Highly stable output pulse timing, spectral bandwidth, and central FEL wavelength.

Upgrade options would allow possible HHG seeding (High Harmonic Gain) or reconfiguration to an EEHG design (Echo-Enabled Harmonic Generation) in order to reach output photon energies of 1.2 keV or greater. EEHG design has been discussed in a separate technical note [2].

2 Two-Stage HGHG

As with the standard LCLS-II design, the electron beam is produced by the high repetition rate, high-brightness, RF photocathode gun and accelerated by the superconducting CW linear accelerator. Relative to the SASE configuration, an HGHG FEL requires smaller energy spread; moreover, the fresh bunch technique needs a relatively long bunch, generally a factor of at least 2.5 greater than the seed laser pulse length. We therefore choose a lower peak current (500 A) than the baseline LCLS-II peak current (1 kA) and a smaller incoherent energy spread (250 keV versus 500 keV). For a 100 pC bunch charge, the usable portion of the bunch length is about 50 μm FWHM. Higher charge options (up to 300 pC) for higher peak current and/or longer bunch duration are possible but are not considered here. The electron beam parameters assumed for this HGHG study are summarized in Table 1.

Table 1. Final electron beam parameters for a possible HGHG FEL.

Parameter	**Value**	**Unit**
Final electron energy	4	GeV
Peak current	500	A
Slice energy spread (rms)	250	keV
Normalized emittance (*x* & *y*)	0.45	μm
Bunch length (FWHM)	50	μm
Bunch repetition rate	100	kHz

The two-stage, HGHG LCLS-II design (see Figure 1) is based on the FEL-2 configuration presently operating successfully at FERMI in Trieste [1]. Each stage includes a "modulator" undulator, a dispersive chicane, and a "radiator" undulator. Between the two stages is a delay chicane; for LCLS-II this would require an equivalent R_{56} of approximately 100 microns or less. Beginning with a 70 fs (FWHM), 300 MW peak power external laser pulse at 210 nm, the first stage is run at a harmonic upshift ratio of 15 to reach 14 nm output with a peak power of 700 MW. After passing through the delay section, second modulator, and dispersive section, the electrons enter a second radiator section consisting of eight LCLS-II baseline SXR undulator segments that produce 2 GW of peak power at a final resonant wavelength of 2 nm (see Figure 2 and left plot of Figure 3). Details of the undulator parameters and required section lengths are given in Table . Our initial time-dependent simulations show that for an idealized electron beam (*e.g.*, temporally flat current and energy) and external laser (perfect Gaussian temporal profile with no phase noise), the spectral output is within a factor of two of the transform limit for a Gaussian pulse (see right plot of Figure 3). The undulator beamline, including chicanes and break sections, required to attain saturation of 2 nm output wavelength is about 60 m. Additional final radiator sections can be used to extract more FEL pulse energy or to accommodate seeded FEL operations at shorter wavelengths.

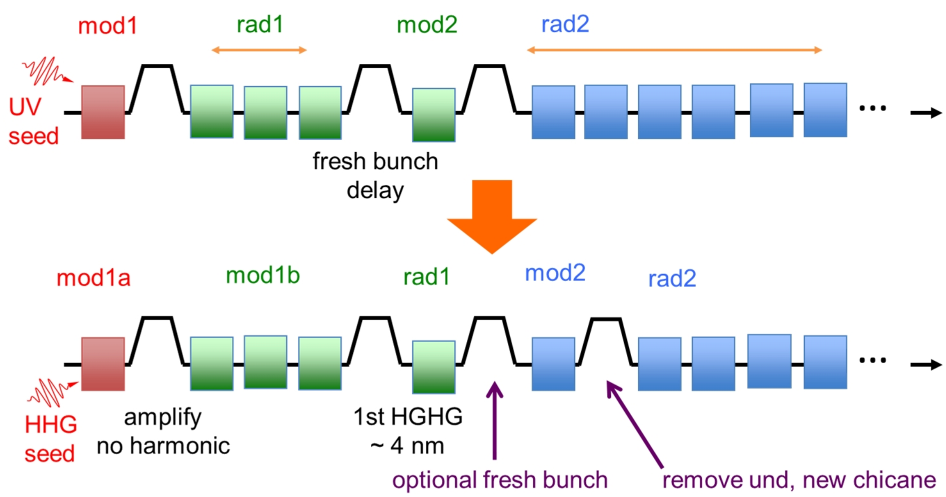

Figure 1. Schematic layout of a two-stage HGHG seeded by a UV laser at 210 nm (upper plot) and a second rebuild-option configured with an HHG laser at 30 nm (lower plot).

Table 2. Undulator parameters.

Parameter	Value	Unit
Mod1 polarization	linear	-
Mod1 period	15	cm
Mod1 K	< 20.6	-
Mod1 resonant wavelength	< 261	nm
Mod1 length	4.5	m
Rad1 and Mod2 polarization	circular/linear	-
Rad1 and Mod2 period	7.5	cm
Rad1 and Mod2 K (rms)	< 8	-
Rad1 and Mod2 resonant wavelength	< 40	nm
Rad1 and Mod2 segment length	3.4	m
Rad2 polarization	linear	-
Rad2 period	3.9	cm
Rad2 K	2.07-5.5	-
Rad2 resonant wavelength	1-5	nm
Rad2 segment length	3.4	m

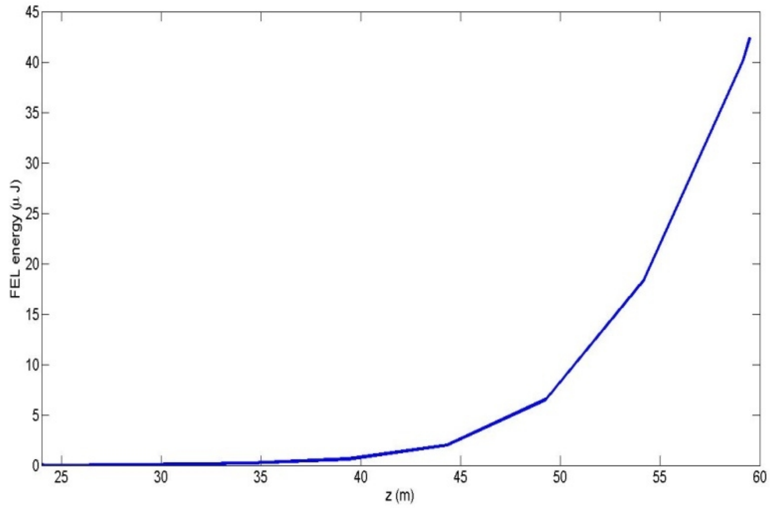

Figure 2. Seeded FEL pulse energy (up to 40 μJ) at 2 nm radiation wavelength along the final radiator ("rad2"). Here *z*=0 marks the beginning of the first stage's modulator ("mod1").

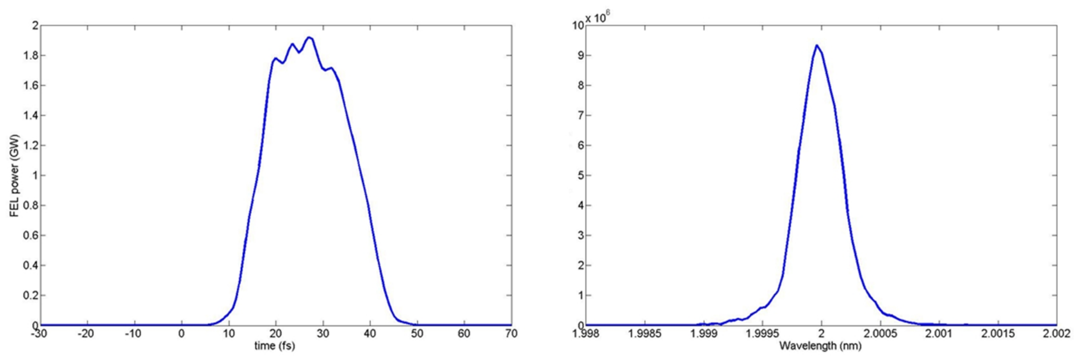

Figure 3. *Left*: Simulated 2 nm FEL power profile at *z*=60 m showing a 25 fs FWHM X-ray pulse duration. *Right*: Corresponding spectral content of the X-ray pulse shows 2x10^{-4} relative bandwidth (FWHM).

3 HHG Modification

The HHG beamline uses almost the same configuration as the two-stage HGHG beamline described above (see Figure). One undulator section in the final radiator can be replaced by a chicane, or, alternatively, the beamline could already have an extra chicane in it. However, the various undulator sections and chicanes will be repurposed. While the beamline still uses two stages of HGHG with a fresh-bunch delay section in between, the harmonics targeted will be much more modest to reach 1 nm wavelength, which would be very challenging when starting with a UV laser as a seed. The HHG laser seeding will begin with a harmonic component of roughly 30 nm wavelength. A peak power of approximately 5 MW and a pulse duration of about 20 fs FWHM for the HHG seed are assumed.

Besides having more modest harmonic jumps and the possibly of extending to shorter wavelengths, the main difference between the HHG beamline and the UV-seeded HGHG configuration is that the 30 nm radiation is amplified using an optical klystron (OK) configuration instead of using a single undulator section for modulation. The first undulator section generates a weak modulation, which is then followed by the first chicane, which generates moderate bunching leading to significant radiation and modulation in the following three undulator sections. This OK configuration makes the HHG seeding less sensitive to initial power requirement. The first stage harmonic upshift is 8, and the second stage harmonic upshift is 4. At about 75 m of the beamline distance, the output pulse energy at 0.94 nm radiation wavelength is more than 20 μJ (see Figure 4). The output pulse at 0.94 nm has a duration of about 15 fs FWHM, with the relative bandwidth of about 3×10^{-4}, about three times the transform limit (see Figure 5).

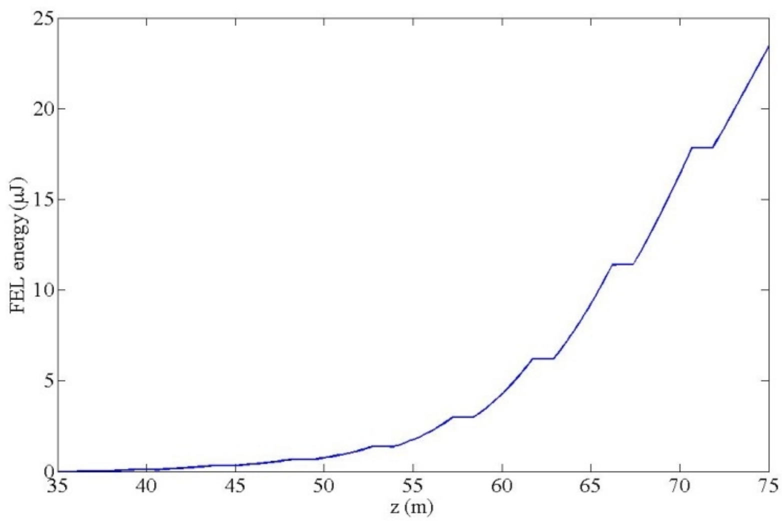

Figure 4. Seeded FEL pulse energy at 0.94 nm radiation wavelength along the final radiator ("rad2"). Here *z*=0 marks the beginning of the first modulator ("mod1").

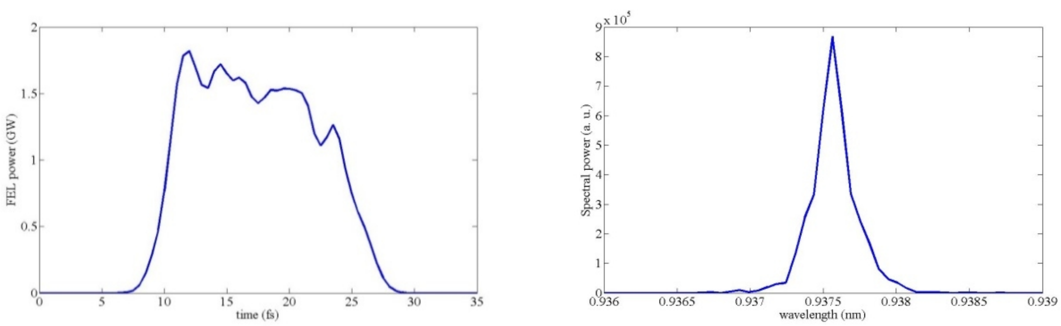

Figure 5. *Left*: Simulated 0.94 nm FEL power profile at *z*=75 m showing a 15 fs FWHM X-ray pulse duration. *Right*: Corresponding spectral content of the X-ray pulse shows $3\text{x}10^{-4}$ relative bandwidth (FWHM).

References

[1] E. Allaria, et al. Nature Photon. **7**, 913–918 (2013).

[2] G. Penn, LCLSII-TN-14-14, 2014.